

See discussions, stats, and author profiles for this publication at: <https://www.researchgate.net/publication/50350221>

Physical Properties at the Base for the Development of an All-Atom Force Field for Ethylene Glycol

ARTICLE *in* THE JOURNAL OF PHYSICAL CHEMISTRY B · MARCH 2011

Impact Factor: 3.3 · DOI: 10.1021/jp109914s · Source: PubMed

CITATIONS

12

READS

39

2 AUTHORS:



Borys Szefczyk

Wroclaw University of Technology

25 PUBLICATIONS 340 CITATIONS

SEE PROFILE



Natália D. S. Cordeiro

University of Porto

245 PUBLICATIONS 3,049 CITATIONS

SEE PROFILE

Physical Properties at the Base for the Development of an All-Atom Force Field for Ethylene Glycol

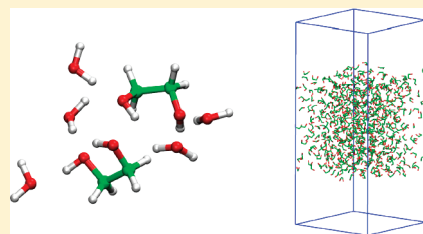
Borys Szeferczyk^{*,†,‡} and M. Natália D. S. Cordeiro[†]

[†]REQUIMTE, Department of Chemistry and Biochemistry, Faculty of Science, University of Porto, Rua Campo Alegre 687, 4169-007 Porto, Portugal

[‡]Institute of Physical and Theoretical Chemistry, Department of Chemistry, Wrocław University of Technology, Wybrzeże Wyspiańskiego 27, 50-370 Wrocław, Poland

S Supporting Information

ABSTRACT: Ethylene glycol, the simplest of the diols, is a popular solvent, an antifreeze agent, a coolant, and a precursor in polymer production. In molecular modeling it is a model compound used to develop potentials for complex systems, like sugars. Despite the fact that many force fields for ethylene glycol exist in the literature, only few of them have been designed to reproduce the macroscopic properties of glycol and its mixtures, and rather more attention has been paid to the microscopic structure of the liquid. Those potentials that reproduce the properties accurately, apply also nonstandard fudge factors, therefore are not fully compatible with any popular force field. In this paper, we present a new potential for ethylene glycol, based on the OPLS all-atom force field and fully compatible with it, as well as with popular models for water. This potential is carefully validated against a broad range of physical properties measured experimentally and published in the literature. These properties include the density, expansion coefficient, compressibility, enthalpy of vaporization, surface tension, self-diffusion coefficient, and viscosity. Therefore, the potential presented here may be used in simulations of not only pure glycol but also mixtures with water, organic solvents, ionic liquids, phase interfaces, etc.



1. INTRODUCTION

Ethylene glycol (1,2-ethanediol), the simplest of the diols, has a vast number of applications in technology, chemistry, and chemical engineering. It is commonly used as a solvent, as well as an antifreeze agent and coolant; and it is a precursor in production of poly(ethylene glycol), PEG, a polymer commonly used for biocompatibility purposes and nanoparticle stabilization.¹ Recently, it has been also applied as a component of ionic liquids (ILs).^{2,3} In molecular modeling, the glycol molecule is used as a template to develop force fields for more complex systems with vicinal hydroxyl groups, like sugars for example.⁴ As a result, several force fields for glycol have been developed and published.^{5–7} In this work, we focus our attention on those compatible with the all-atom OPLS force field,⁸ commonly used to simulate molecular liquids, including ionic liquids.⁹ It has to be mentioned that both the all-atom and the united-atom force fields exist;^{5,7} however, here we restrict our attention to the all-atom force fields only. Unfortunately, most of the OPLS-AA-based force fields for glycol were developed to reproduce the microscopic structure of the liquid (e.g., equilibrium between *trans* and *gauche* conformers)^{6,10} or to design force fields for biological molecules, like sugar.^{4,11} This came at the sacrifice of the ability to reproduce the physical properties of the liquid glycol itself. In the OPLS-AA force field, nonbonding interactions between atoms separated by three bonds (1–4 interactions) are scaled. The standard scaling factor is 0.5 for both

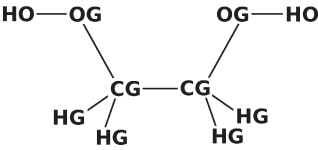
Coulomb and Lennard-Jones interactions. For the glycol molecule, it has been proposed to use different scaling factors^{5,6} or even apply an extra scaling factor for the interaction between atoms separated by four bonds (1–5 interactions).⁴ Although this approach has been found to improve the quality of the force field, it is somewhat troublesome, when the force field is used for mixtures. Namely, molecular dynamics packages like GROMACS¹² usually permit us to define only a single scaling factor for the whole system in a convenient way. This can be problematic if the goal of the study is to simulate complex systems, like ILs (e.g., composed of glycol and choline chloride)² or mixtures, e.g., with other alcohols.¹³ Therefore, in our work we attempt to optimize the force field for liquid glycol, with the following two requirements in mind: (i) the physical properties of liquid glycol, like density, thermal expansion, compressibility, heat of vaporization, and surface tension, should be reproduced as good as possible and (ii) the force field should be kept as simple as possible, without introducing “exotic” parameters and maintaining full compatibility with the OPLS-AA force field. Such a force field should be robust and easily combined with other compounds. We also pay attention to the interaction of ethylene glycol with water in aqueous solutions; these kinds of

Received: October 15, 2010

Revised: February 15, 2011

Published: March 09, 2011

Table 1. Optimized Charges and Lennard-Jones Parameters

			
type	charge	σ [Å]	ϵ [kcal mol ⁻¹]
CG	0.165	3.50	0.066
HG	0.060	2.50	0.030
OG	-0.720	3.00	0.170
HO	0.435	0.00	0.000

mixtures are interesting due to the fact that the hydrogen bonding with the solvent may compete with the intramolecular hydrogen bond present in the glycols.¹⁴ Therefore, we test the performance of our potential in conjunction with two popular water models, the Simple Point Charge/Extended model, SPC/E,¹⁵ and the Transferable Intermolecular Potential (4-point) model, TIP4P.¹⁶

This paper is organized as follows: in the next section, we describe the parametrization of the force field, the setup of the molecular dynamics simulations, and how the different properties were evaluated; in section 3, we discuss the different aspects of the parameter optimization and performance of the force field, compared to the experimental properties; finally, our main conclusions are summarized in the last section.

2. METHODS

2.1. Parametrization. The parameters of glycol are based on the original parameters for alcohols and organic molecules published by Jorgensen et al.^{8,17} The bonded interactions, bonds and angles (except for the dihedrals), were left unchanged. As in the original force field, we maintain the scaling factors of 0.5 for 1–4 Coulomb and van der Waals interactions; 1–2 and 1–3 nonbonded interactions (Coulomb and Lennard-Jones) are excluded, as they are already described by the harmonic potentials. The atomic charges were obtained in the following way: the glycol molecule was optimized at the RHF/6-31G(d) level, and after that, a single-point calculation was done at the MP2 level using the aug-cc-pVTZ(-f) basis set (f-type functions were skipped). Charges were fitted to reproduce the electrostatic potential on a grid generated using the CHELPG algorithm.¹⁸ This is an established procedure, used to develop OPLS-type force fields. Next, the charges were rounded up, symmetrized, and assigned to atoms. Finally, they were changed by hand to reproduce physical properties of liquid glycol at ambient conditions. This was necessary since the ground-state point charges calculated in vacuum do not represent well the charge distribution of the molecule in liquid and in other than ground-state conformation. Such a procedure is typical for the OPLS force field.¹⁷ It is known¹⁹ that this kind of procedure is very difficult to automate; therefore, we have proceeded with a more tedious, manual (based on chemical intuition) procedure of changing the parameters and recalculating the properties, until they were satisfactorily reproduced in the simulation. Final charges are listed in Table 1 (the atom symbols are shown as well).

Table 2. Dihedral Angle Parameters

dihedral	V_1	V_2	V_3
	[kJ/mol]		
OG–CG–CG–OG	12.521	–2.736	11.800
CG–CG–OG–HO	1.656	–3.139	4.300

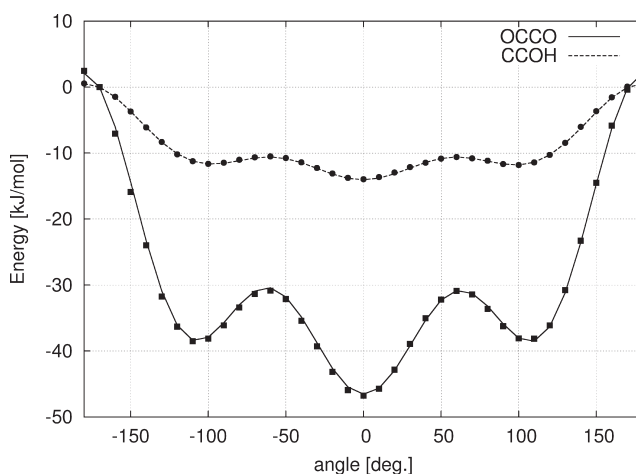


Figure 1. Profiles of the two dihedral angles plotted using the optimized parameters: symbols, quantum chemical (RHF/6-31G(d)) energy; lines, force field energy.

The original Lennard-Jones parameters were mostly maintained, except for the hydroxyl group oxygen van der Waals radius. For the oxygen atom in the hydroxyl group, different values of the radius (σ) are used, ranging from 3.07 to 3.18 Å.^{7,11} Our tests indicate that none of these values can reproduce the properties satisfactorily. The radius has been therefore shortened further, to the value of 3.00 Å, and the charge optimization has been continued. All the Lennard-Jones parameters used are listed in Table 1.

Finally, the dihedral angle parameters were always reoptimized after changing the charges or the van der Waals radius, to reproduce exactly the energy profiles calculated using the quantum mechanical method. The OPLS-AA force field uses the Fourier form of the dihedral potential

$$V_{\phi} = \frac{1}{2}[V_1(1 + \cos \phi) + V_2(1 - \cos 2\phi) + V_3(1 + \cos 3\phi)]$$

In the fitting procedure, the two dihedral angles present in the molecule, O–C–C–O and C–C–O–H, were stepped by 10° in the full-angle range. The RHF/6-31G(d) energy was calculated for each conformer, and fitting was performed. The rest of the molecule was kept fixed during the scan (it was not relaxed). The Fourier coefficients were optimized to minimize the square difference of barriers of rotation

$$\sum_{\alpha} (\Delta E_{\text{ff}}(\alpha) - \Delta E_{\text{QM}}(\alpha))^2 = \min$$

where $\alpha = -180, -170, \dots, 170$; E_{QM} is the energy calculated at the Hartree–Fock level; and E_{ff} is the sum of intramolecular terms

$$\Delta E_{\text{ff}} = \Delta E_{\text{eq}} + \Delta E_{\text{vdW}} + \Delta E_{\text{dih}}$$

where E_{qq} is the Coulomb intramolecular interaction; E_{vdW} is the intramolecular interaction; and E_{dih} is the optimized dihedral term. Final values of the dihedral parameters are listed in Table 2, and the profiles are shown in Figure 1.

The complete force field in the GROMACS topology format can be found in the Supporting Information. Note that GROMACS uses SI units (distance is measured in nanometers), and bond and angle harmonic potentials have an additional 0.5 factor, which doubles the force constants. Also, dihedral angles are expressed as Ryckaert–Bellemans functions. Therefore, the numerical values of the parameters in the attached topology file differ from those presented in this paper.

2.2. System Setup and Molecular Dynamics. The initial system was constructed by inserting 560 glycol molecules into a box, at random positions. The size of the box was approximately $3.6 \times 3.6 \times 4.0$ nm. Periodic boundary conditions (PBCs) were applied in all simulations. The system prepared for viscosity calculations used a box elongated in the z direction ($L_z = 3L_x = 3L_y = 9.4$ nm). All calculations were done using the GROMACS 4 package¹² and the developed force field, compatible with the already implemented OPLS-AA force field. The systems were initially optimized using the steepest-descent method, until all forces decreased below the 500 kJ/(mol nm) threshold. The short-range Coulomb interactions were calculated within 1.2 nm cutoff, and the short-range van der Waals interactions were calculated within 1.4 nm cutoff. Long-range Coulomb interactions were computed using the particle-mesh Ewald method with 0.12 nm spacing of the grid points in the reciprocal space. The short-range interaction lists were updated every 10 steps, using a grid-based method. The Nosé–Hoover thermostat^{20,21} was used in the NVT and NPT ensembles, and the Parrinello–Rahman barostat²² was applied in the NPT ensemble. The production runs were performed with a time step of 2 fs, with all bonds constrained using LINCS algorithm.²³ Every 5 steps translation of the center of mass was removed. Errors were estimated by dividing the production run into 200 ps blocks and calculating averages and standard deviations for those blocks. The errors were computed at the confidence interval of 95%.

Mixtures with water have been simulated in systems consisting of 315 glycol molecules and 473 water molecules in a box of roughly $3.5 \times 3.5 \times 3.5$ nm. For the calculations of viscosity, the number of molecules have been doubled, and the box has been elongated in the z -direction (again, $L_z = 3L_x = 3L_y$). Two popular water models have been tested: the SPC/E¹⁵ and the TIP4P.¹⁶ Other parameters of the simulations equal those used for pure glycol (see above).

2.3. Physicochemical Properties. Several static- and transport properties of liquid glycol were evaluated from the molecular dynamics simulations in order to assess the quality of the developed force field. These properties were compared with the experimental data.

Density (ρ) at different temperatures was obtained by averaging the results from 3 ns NPT simulations. Pressure in these simulations was maintained at 1 bar. The 3 ns period was divided into 200 ps blocks to estimate the errors. The results were compared with experimental²⁴ density ρ_{exp} given by

$$\rho_{\text{exp}} = 1.1257 - 0.5713 \times 10^{-3}T - 2.776 \times 10^{-6}T^2 + 10.9 \times 10^{-9}T^3 \quad (1)$$

where T is temperature in °C.

Thermal expansion coefficient (α_p) was estimated from the density at 298 and 373 K, using the numerical derivative

$$\alpha_p = \frac{1}{V} \left(\frac{\partial V}{\partial T} \right)_p \approx - \left(\frac{\ln \left(\frac{\rho_2}{\rho_1} \right)}{T_2 - T_1} \right)_p \quad (2)$$

and compared with the experimental value, calculated from the slope of the density function (eq 1).

Isothermal compressibility (β_T) was calculated as the numerical derivative of the volume with respect to the pressure

$$\beta_T = - \frac{1}{V} \left(\frac{\partial V}{\partial P} \right)_T \approx \left(\frac{\ln \left(\frac{\rho_2}{\rho_1} \right)}{P_2 - P_1} \right)_T \quad (3)$$

For that purpose, two 3 ns NPT simulations have been performed at 298 K and at 1 and 100 bar. The compressibility has been also estimated from the fluctuations of the volume of the system simulated at 298 K and 1 bar

$$\beta_T = \frac{\langle \delta V^2 \rangle_{\text{NPT}}}{Vk_B T} \quad (4)$$

The results were compared with experimental β_T obtained from ultrasound velocity measurements.¹³

Enthalpy of vaporization (ΔH_{vap}) was calculated using the approach proposed by Jorgensen.²⁵ This approach assumes that the sum of vibrational and kinetic energies is equal for the gas and liquid phase. The enthalpy of vaporization might be then written as

$$\Delta H_{\text{vap}} = E_{\text{dih}}(\text{g}) + E_{\text{intra}}(\text{g}) - [E_{\text{dih}}(\text{l}) + E_{\text{intra}}(\text{l}) + E_{\text{inter}}(\text{l})] + RT$$

Subscripts g and l refer to the gas and liquid phase, respectively; E_{dih} is the dihedral energy term; E_{intra} is the nonbonding intramolecular interaction energy; and E_{inter} is the intermolecular interaction energy. Experimental values of ΔH_{vap} are within the range 63–68 kJ mol^{−1}, depending on the technique used.²⁶

Enthalpy of solvation (ΔH_{sol}^0) was computed according to the formula²⁷

$$\Delta H_{\text{sol}}^0 = \langle U_{\text{sw}} \rangle + \langle U_{\text{rel}} \rangle - RT$$

where $\langle U_{\text{sw}} \rangle$ is the solute–water interaction energy, and $\langle U_{\text{rel}} \rangle$ is the water–water relaxation energy due to removal of the solute. Both quantities are calculated from NVT runs at 298.15 K, one with a single glycol molecule solvated by 890 water molecules and the second with glycol removed.

Surface tension (γ) was estimated from a simulation performed with the initial box extended to 8 nm in the z direction, so that the periodic images of the liquid in this direction were separated by ca. 3.5 nm of vacuum. Such a system was equilibrated and simulated in the NVT ensemble for 3 ns, collecting the components of the pressure tensor. Next, the surface tension was estimated using the formula²⁸

$$\gamma_V = \frac{1}{2}L_z \left(\langle P_{zz} \rangle - \frac{\langle P_{xx} \rangle + \langle P_{yy} \rangle}{2} \right)$$

The factor 1/2 is due to the presence of two interfaces in the system.

Shear viscosity (η) has been calculated according to the nonequilibrium periodic perturbation method.²⁹ A 3 ns NVT simulation has been performed, in a box elongated in the z direction and a periodic acceleration $a_x(z)$ applied along the x axis

$$a_x(z) = A \cos\left(\frac{2\pi}{L_z} z\right)$$

with L_z being the length of the box in the z direction and A being an arbitrary amplitude parameter. This parameter has been fine-tuned manually (to achieve good statistics and yet to prevent the system diverging too far from the equilibrium). The value of A used in the simulations was 0.005 nm ps^{-2} . The shear viscosity η is calculated from the velocity profile (v)

$$\eta = \frac{A\rho}{v} \left(\frac{L_z}{2\pi}\right)^2$$

Technical aspects of this approach have been described more extensively elsewhere.³⁰

Self-diffusion coefficient (D) was estimated from a 3 ns NVT simulation, based on the Einstein relation (root-mean-square displacement)

$$D = \frac{1}{6t} \langle |\vec{r}_i(t) - \vec{r}_i(0)|^2 \rangle \quad (5)$$

The average $\langle \dots \rangle$ is over all the molecules in the system and over several restarts $\vec{r}_i(0)$ spaced every 10 ps along the trajectory.

3. RESULTS

The optimization procedure used here has focused on reproducing the macroscopic physicochemical properties of ethylene glycol, and therefore the parameters that have been changed are those responsible for intermolecular interactions: charges and van der Waals parameters. The dihedral angles also influence some of the properties (although in a minor degree) and have been tuned in the last stage of the optimization to keep the proper conformation distribution. In general, the optimization was based on repeating three steps in the following order: (i) changing the Coulomb point charges, (ii) changing the van der Waals radii (only hydroxyl oxygen), and (iii) refitting the dihedrals. Compared to the OPLS force field,⁸ the charge on the hydrogen in the hydroxyl group is preserved, whereas some additional charge is transferred from the methylene group to the oxygen, resulting in an increased negativity of the latter. The hydroxyl group is more polarized than in the OPLS-AA force field,¹⁷ where the charge on the oxygen atom is -0.683 ; however, these parameters were developed for monofunctional alcohols. When vicinal hydroxyl groups are present, higher charges are required.⁴ Optimized charges can be found in Table 1. Also, the van der Waals radius of the hydroxyl oxygen is reduced, compared to other force fields (Table 1). In our model, only three dihedral angles are present, one for the O–C–C–O angle and two for the C–C–O–H angles. Parameters of these angles have been reoptimized to fit the rotation barrier, calculated at the RHF/6-31G(d) level of theory. The barriers were calculated for each type of dihedral separately, keeping the structure fixed and stepping only the dihedral angle. We have found this procedure more convenient and reliable than a relaxed scan of the rotation barrier (i.e., including energy minimization at each point), probably because keeping the structure fixed allows us to isolate the effects due to the dihedral angle from other interactions in the system.

Table 3. Physical Parameters of Ethylene Glycol at 298.15 K and 1 bar (If Not Stated Otherwise)^a

quantity	unit	calculated	experimental	
ρ	$\text{kg} \cdot \text{m}^{-3}$	1109.6 ± 0.9	1110	24
ρ , 100 °C	$\text{kg} \cdot \text{m}^{-3}$	1038.7 ± 0.7	1052	24
ΔH_{vap}	$\text{kJ} \cdot \text{mol}^{-1}$	75.65 ± 0.05	63 – 68	26
β_T	10^{-5} bar^{-1}	5.39 ± 1.20^b	3.34	13
		4.15 ± 0.32^c		
α_p	10^{-4} K^{-1}	8.81 ± 0.14	6.7^d	24
D	$10^{-6} \text{ cm}^2 \cdot \text{s}^{-1}$	1.5 ± 0.1	0.9	34
γ , 20 °C	$\text{mN} \cdot \text{m}^{-1}$	50.8 ± 4.5	47.7 – 49.1	24,35
η	$\text{cP}, \text{ mPa} \cdot \text{s}$	8.3 ± 1.2	16	24

^a References are given in the last column. ^b Based on the numerical derivative, eq 3. ^c Based on the volume fluctuation eq 4. ^d Calculated from the slope of the density vs temperature, eq 1.

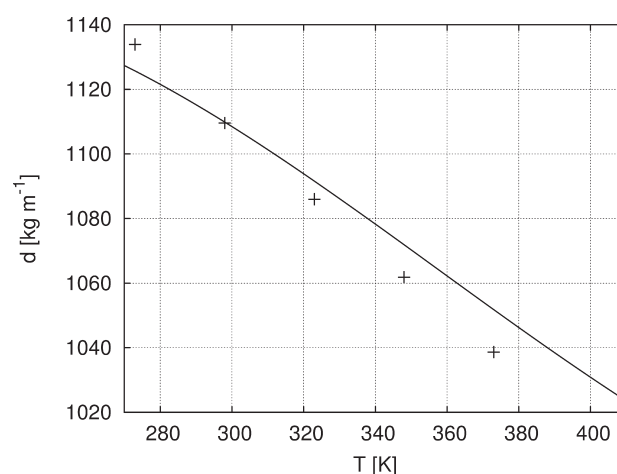


Figure 2. Density of ethylene glycol at various temperature. Solid line, experimental density, based on eq 1; points, calculated density.

The developed potential reproduces accurately the room-temperature density of glycol. The thermal expansion coefficient, $8.81 \times 10^{-4} \text{ K}^{-1}$, is slightly overestimated compared to the experimental value (Table 3), so that the density-versus-temperature curve has a bit higher slope than the experimental one (eq 1 and Figure 2). Also, the isothermal compressibility is slightly overestimated: both the numerical estimate, $5.4 \times 10^{-5} \text{ bar}^{-1}$, and the estimate based on volume fluctuation, $4.1 \times 10^{-5} \text{ bar}^{-1}$, are higher than the experimental value (Table 3). Surface tension and enthalpy of vaporization are in good accordance with experiment; however, in both cases the calculated value is higher than the experimental one, which can indicate too strong intermolecular interactions. The dynamic properties, viscosity, and self-diffusion are reproduced less accurately; i.e., the viscosity is too low, and the self-diffusion coefficient is overestimated, indicating that the mobility of the glycol molecules might be still too high. Considering the fact that the compressibility and the expansion coefficient are second-order properties, the observed discrepancies (compared to the experiment) are not large. Also the transport properties, like the viscosity, are usually difficult to estimate, both experimentally and from simulations. Concerning the viscosity, the nonequilibrium method applied here includes an arbitrary parameter, i.e., the amplitude of the induced fluctuations, A . If this parameter is set too low, the statistics on

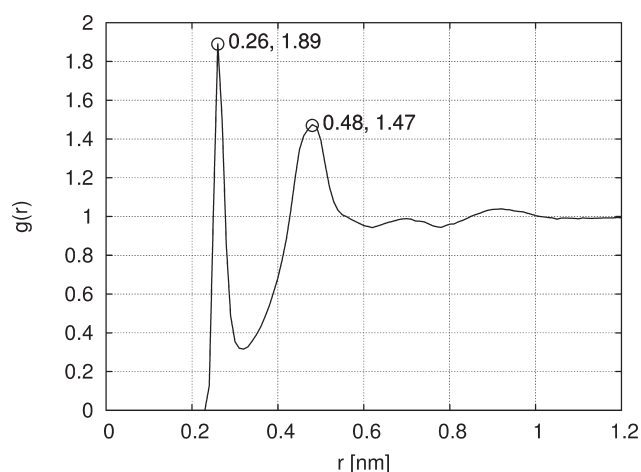


Figure 3. Radial distribution function of the oxygen–oxygen distance in pure liquid ethylene glycol at 298.15 K and 1 bar.

Table 4. Properties of Ethylene Glycol at 298.15 K and 1 bar Calculated Using Various Force Fields Available from the Literature: (A) OPLS-AA,^{8,17} (B) Force Field Developed for Sugars,⁴ and (C) an All-Atom Potential by Gubskaya and Kusalik⁵

property	unit	A	B	C	this work	experimental	
ρ	$\text{kg}\cdot\text{m}^{-3}$	1047.0	1068.0	1083.0	1110.0	1110	24
β_T	10^{-5} bar^{-1}	4.9	4.2	5.0	5.4	3.3	13
α_p	10^{-4} K^{-1}	10.1	9.5	8.6	8.8	6.7	24
D	$10^{-6}\text{ cm}^2\cdot\text{s}^{-1}$	5.5	4.4	2.2	1.5	0.9	34
ΔH_{vap}	$\text{kJ}\cdot\text{mol}^{-1}$	59.2	64.3	72.2	75.6	63 – 68	26

the velocities are poor; if it is too high, the system might diverge too far from equilibrium. For that reason, it is customary to try different values of A ; here, we have tested $A = 0.002, 0.005$, and 0.010 nm ps^{-2} . We did not observe a significant dependence of the viscosity on the amplitude, and the values quoted in the tables are for $A = 0.005$, which gave the smallest statistical errors. Considering the microscopic structure of the ethylene glycol, the Radial Distribution Function (RDF) of the oxygen–oxygen distance shows a peak at 2.6 \AA (Figure 3)—this is a bit shorter distance than the one obtained from the neutron diffraction experiment (2.78 \AA).³¹

Several force fields of glycol have been published and tested in the literature. Some of them, like OPLS and OPLS-AA,^{8,17} are general force fields for alcohols or sugars and can be applied to glycols; others, like the force fields of Saiz et al.,¹⁰ Gubskaya and Kusalik,⁵ Oliveira and Freitas,⁶ and Geerke and van Gunsteren⁷ were designed specifically for ethylene glycol. Many potentials are united-atom models, whereas some groups have published also an all-atom model of glycol.^{5,6} To verify the performance of our model, we compare the properties calculated using three different potentials from the literature: the OPLS-AA force field, the potential developed for sugars by Kony et al., and the all-atom potential proposed by Gubskaya.⁵ It has to be mentioned that the all-atom model presented in the latter paper was discarded by the authors since the united-atom model presented in the same paper gave better results. We refer to this all-atom model only to be consistent, and use the same ten-center representation in all models. Table 4 shows that all potentials display similar values of

Table 5. Properties of Ethylene Glycol ($x = 0.4$):Water ($x = 0.6$) Mixture at 293.15 K and 1 bar^a

property	unit	SPC/E	TIP4P	expt.	
ρ	$\text{kg}\cdot\text{m}^{-3}$	1090.0	1091.0	1088.0	35
γ	$\text{mN}\cdot\text{m}^{-1}$	58.0	55.6	55.0	35
η	cP, $\text{mPa}\cdot\text{s}$	6.0	4.3	6.8	35
β_T	10^{-5} bar^{-1}	4.44	3.73	3.33	36
ΔH_{sol}^0	$\text{kJ}\cdot\text{mol}^{-1}$	−110.1	−105.1	−74.5	37
D	$10^{-6}\text{ cm}^2\cdot\text{s}^{-1}$	1.7	2.3	4.2 − 5.5	38

^aThe enthalpy of solution is at 298.15 K and at infinite dilution. Reference for the experimental value is given in the last column.

isothermal compressibility, slightly overestimated compared with experiment. The thermal expansion coefficient is also overestimated; however, the potential developed in this work and the one by Gubskaya and Kusalik are the closest to the experimental value. This will lead to systematically underestimated density, which is already significantly underestimated at room temperature, in all models except the one developed in this paper. Therefore, our potential gives the best estimate of this basic property. The OPLS force field underestimates the enthalpy of vaporization, and our model as well as the model developed by Gubskaya and Kusalik overestimate it. Only the force field by Kony et al. falls into the range of experimental values. All models suffer from overestimated self-diffusion coefficients; however, our model is already close to the experimental value. Concluding, we believe that our model gives the most accurate description of the density and dynamic properties over a range of temperatures.

The potential developed in the present work is supposed to perform equally well for pure glycol and in mixtures; therefore, we test its behavior in conjunction with two models of the most popular solvent, water. Experimental values of the density, surface tension, enthalpy of solvation, viscosity, and isothermal compressibility have been used to validate the potential. Table 5 shows that with both models, SPC/E and TIP4P, most properties are described very well; the only discrepancies are that, in the model system with SPC/E water, the compressibility and surface tension are slightly overestimated, whereas the model with TIP4P underestimates the viscosity. It has to be remembered, however, that the transport properties such as viscosity and the second-order properties (compressibility) are usually more difficult to reproduce. The table shows also the enthalpies of solvation, which are overestimated, compared to the experimental value. We have found that the potential proposed by Gubskaya and Kusalik⁵ results in a value much closer to the experiment, although still overestimated (calc. $\Delta H_{\text{sol}}^0 = -88.8 \text{ kJ/mol}$ vs expt. $\Delta H_{\text{sol}}^0 = -74.5 \text{ kJ/mol}$).

Finally, it has to be mentioned that we observed some dependence of the properties on the cutoff radii. Although it is well-known that the cutoff lengths influence certain properties calculated from MD simulations,^{32,33} these important parameters are often neglected or even not mentioned in publications. For the potential presented here, it is therefore recommended that the same (or similar) cut-offs are used, namely, 1.4 nm for the van der Waals interactions and 1.2 nm for the Coulomb interactions. When other cut-offs are applied, the potential should be probably validated again.

As it has been mentioned in section 2, this potential uses only the standard scaling parameters for 1–4 Coulomb and van der Waals interactions (so-called fudge factors). It has been

suggested that for glycol and vicinal alcohols other scaling parameters have to be used^{5,6} or even that 1–5 and 1–6 interactions have to be scaled as well.⁴ The glycol molecule does not contain 1–6 interaction, and in our model the only 1–5 interactions present are those between hydrogen and oxygen in the opposite hydroxyl groups. Since the van der Waals parameters for these hydrogens are set to zero, the scaling would not affect them. The 1–5 Coulomb interaction on the other hand is nonzero, but we did not find the need to scale this interaction.

4. CONCLUSIONS

In this work, a new potential for 1,2-ethylene glycol has been developed. This potential is based on the OPLS-AA force field and is fully compatible with the original parameter sets. It has been also shown that the potential can be used with popular standard water models, like SPC/E or TIP4P. In opposition to other published parameter sets, this potential uses only standard scaling factors for van der Waals and Coulomb 1–4 interactions, which makes it particularly attractive for applications requiring mixing of different parameter sets. The potential has been developed to match experimentally determined properties of liquid in ambient conditions (atmospheric pressure and room temperature); however, it reproduces experimental densities quite well also at higher temperatures. The force field has been validated using a number of static and transport properties, such as: the density, expansion coefficient, isothermal compressibility, enthalpy of vaporization, surface tension, self-diffusion coefficient, and viscosity. The physical parameters of a mixture with water have been also calculated and have proven that the force field performs well. The potentials describing the dihedral angles have been fitted carefully to quantum chemical profiles. It has to be stressed that the physical properties depend on those properties, due to the different number of hydrogen bonds that can be formed between various rotamers of the glycol molecule.¹⁰ Comparison with other available force fields shows that in fact some progress has been achieved, and to the best of our knowledge, this potential predicts some experimental observables better than other force fields of the same kind (i.e., force fields compatible with OPLS-AA). Although we do not find the need for using nonstandard fudge factors, neither for scaling 1–5 Coulomb interactions—about the 1–5 vdW—we do not conclude, as they are not present in our system. It is likely that they might be still necessary in other glycols and compounds with several vicinal hydroxyl groups, like triols or sugars.

■ ASSOCIATED CONTENT

S Supporting Information. Ethylene glycol topology and parameter set in GROMACS format. This material is available free of charge via the Internet at <http://pubs.acs.org>.

■ ACKNOWLEDGMENT

This work is supported by the project PTDC/EQU-FTT/104195/2008 funded by FCT, Lisbon, Portugal. B. Szeferczyk would like to thank FCT (Lisbon, Portugal) for the fellowship funded within the Ciencia2008 programme. Calculations have

been carried out at Wroclaw Centre for Networking and Supercomputing (WCSS), Wroclaw, Poland.

■ REFERENCES

- (1) Yoo, J.-W.; Chambers, E.; Mitragotri, S. *Curr. Pharm. Des.* **2010**, *16*, 2298–2307.
- (2) Abbott, A. P.; Harris, R. C.; Ryder, K. S. *J. Phys. Chem. B* **2007**, *111*, 4910–4913.
- (3) Lawes, S. D. A.; Hainsworth, S. V.; Blake, P.; Ryder, K. S.; Abbott, A. P. *Tribol. Lett.* **2010**, *37*, 103–110.
- (4) Kony, D.; Damm, W.; Stoll, S.; van Gunsteren, W. F. *J. Comput. Chem.* **2002**, *23*, 1416–1429.
- (5) Gubskaya, A. V.; Kusalik, P. G. *J. Phys. Chem. A* **2004**, *108*, 7151–7164.
- (6) de Oliveira, O. V.; Freitas, L. C. G. *J. Mol. Struct. (THEOCHEM)* **2005**, *728*, 179–187.
- (7) Geerke, D. P.; van Gunsteren, W. F. *Mol. Phys.* **2007**, *105*, 1861–1881.
- (8) Jorgensen, W. L. *J. Phys. Chem.* **1986**, *90*, 1276–1284.
- (9) Sambasivarao, S. V.; Acevedo, O. *J. Chem. Theory Comput.* **2009**, *5*, 1038–1050.
- (10) Saiz, L.; Padró, J. A.; Guàrdia, E. *J. Chem. Phys.* **2008**, *114*, 3187–3198.
- (11) Damm, W.; Frontera, A.; Tirado-Rives, J.; Jorgensen, W. L. *J. Comput. Chem.* **1997**, *18*, 1955–1970.
- (12) Hess, B.; Kutzner, C.; van der Spoel, D.; Lindahl, E. *J. Chem. Theory Comput.* **2008**, *4*, 435447.
- (13) Jerie, K.; Baranowski, A.; Przybylski, J.; Glin'ski, J. *J. Mol. Liq.* **2004**, *111*, 25–31.
- (14) Gubskaya, A. V.; Kusalik, P. G. *J. Phys. Chem. A* **2004**, *108*, 7165–7178.
- (15) Berendsen, H. J. C.; Grigera, J. R.; Straatsma, T. P. *J. Phys. Chem.* **1987**, *91*, 6269–6271.
- (16) Jorgensen, W. L.; Chandrasekhar, J.; Madura, J. D.; Impey, R. W.; Klein, M. L. *J. Chem. Phys.* **1983**, *79*, 926–935.
- (17) Jorgensen, W. L.; Maxwell, D. S.; Tirado-Rives, J. *J. Am. Chem. Soc.* **1996**, *118*, 11225–11236.
- (18) Breneman, C. M.; Wiberg, K. B. *J. Comput. Chem.* **1990**, *11*, 361–373.
- (19) MacKerell, A. D.; et al. *J. Chem. Phys. B* **1998**, *102*, 3586–3616.
- (20) Nosé, S. *Mol. Phys.* **1984**, *52*, 255–268.
- (21) Hoover, W. G. *Phys. Rev. A* **1985**, *31*, 1695–1697.
- (22) Parrinello, M.; Rahman, A. *J. Appl. Phys.* **1981**, *52*, 7182–7190.
- (23) Hess, B.; Bekker, H.; Berendsen, H. J. C.; Fraaije, J. G. E. M. *J. Comput. Chem.* **1997**, *18*, 1463–1472.
- (24) Washburn, E. *International Critical Tables of Numerical Data, Physics, Chemistry and Technology*, 1st Electronic ed.; Knovel: Norwich, New York, 2003.
- (25) Jorgensen, W. L.; Madura, J. D.; Swenson, C. J. *J. Am. Chem. Soc.* **1984**, *106*, 6638–6646.
- (26) Verevkin, S. P. *Fluid Phase Equilib.* **2004**, *224*, 23–29.
- (27) Arroyo, S. T.; Martin, J. A. S.; Garcia, A. H. *Chem. Phys.* **2005**, *315*, 76–80.
- (28) Jorge, M.; Cordeiro, M. N. D. S. *J. Phys. Chem. B* **2008**, *112*, 2415–2429.
- (29) Ciccotti, G.; Jacucci, G.; McDonald, I. R. *J. Stat. Phys.* **1979**, *21*, 1–22.
- (30) Jorge, M.; Gulaboski, R.; Perreira, C. M.; Cordeiro, M. N. D. S. *J. Phys. Chem. B* **2006**, *110*, 12530–12538.
- (31) Bakó, I.; Grós, T.; Pálinkás, G. *J. Chem. Phys.* **2003**, *118*, 3215–3221.
- (32) Yonetani, Y. *J. Chem. Phys.* **2006**, *124*, 204501.
- (33) Sendner, C.; Horinek, D.; Bocquet, L.; Netz, R. R. *Langmuir* **2009**, *25*, 10768–10781.
- (34) Chandrasekhar, N.; Krebs, P. *J. Chem. Phys.* **2000**, *112*, 5910–5914.

- (35) Tsierkezos, N. G.; Molinou, I. E. *J. Chem. Eng. Data* **1998**, *43*, 989–993.
- (36) Uosaki, Y.; Kitaura, S.; Moriyoshi, T. *J. Chem. Eng. Data* **2006**, *51*, 423–429.
- (37) Kulikov, M. V.; Trutneva, E. Y. *Russ. Chem. Bull.* **1997**, *46*, 1518–1525.
- (38) Ternström, G.; Sjöstrand, A.; Aly, G.; Jernqvist, Å. *J. Chem. Eng. Data* **1996**, *41*, 876879.